PROGRESS IN PHOTOVOLTAICS: RESEARCH AND APPLICATIONS
Prog. Photovolt: Res. Appl. 2008; **16**:325–330
Published online 20 November 2007 in Wiley InterScience (www.interscience.wiley.com) DOI: 10.1002/pip.803

Research *SHORT COMMUNICATION*

On The Detection of Shunts in Silicon Solar Cells by Photo- and Electroluminescence Imaging

Otwin Breitenstein[1*,†], Jan Bauer[1], Thorsten Trupke[2] and Robert A. Bardos[2]
[1]*Max Planck Institute of Microstructure Physics, Weinberg 2, D-06120 Halle, Germany*
[2]*Centre of Excellence for Advanced Silicon Photovoltaics and Photonics, University of New South Wales, Sydney, NSW 2052, Australia*

Recently electroluminescence (EL) and photoluminescence (PL) imaging were reported to allow detection of strong ohmic shunts in silicon solar cells. Comparing lock-in thermography (LIT) images with luminescence images of various shunted cells, measured under different conditions, the ability of luminescence techniques for shunt detection is investigated. Luminescence imaging allows identifying ohmic shunts only if they reach a certain strength. The detection limit for PL measurements of linear shunts was estimated to be in the order of 15 mA at 0·5 V bias for a point-like shunt in multicrystalline (mc) cells. Pre-breakdown sites can also be detected by electroluminescence under reverse bias. Copyright © 2007 John Wiley & Sons, Ltd.

KEY WORDS: silicon solar cells; shunt investigation; lock-in thermography; electroluminescence; photoluminescence

Received 7 June 2007; Revised 1 August 2007

Electro- and photoluminescence (EL and PL) imaging have been introduced as very efficient techniques for spatially resolved characterization of silicon solar cells.[1,2] Specifically the localization of strong ohmic shunts in industrial multicrystalline (mc) silicon cells via EL and PL imaging has recently been reported.[3,4,5,6] However, besides ohmic shunts, there are also other types of shunts, like non-linear shunts and pre-breakdown sites.[7] While ohmic shunts show a linear current–voltage (I–V) characteristic and usually also dominate under high reverse bias, the I–V characteristic of non-linear shunts is diode-like, with the higher conductivity in silicon cells always in forward bias direction. Non-linear shunts can be caused by strongly recombination-active defects crossing the pn-junction or by a direct contact of the grid metal to the base (Schottky-type shunts). These non-linear shunts are generally less harmful than ohmic shunts, but they also degrade the fill factor and the low light level performance of solar cells.[8] Pre-breakdown sites show no or only a weak conductivity under low forward and reverse bias, but a strongly increasing conductivity for higher reverse bias above −5 V typically. They are avalanche breakdown sites, caused by defects crossing the pn-junction or other reasons of local high fields. If these pre-breakdown sites show currents of several amperes at reverse voltage of −13 V, they become particularly problematic because in the case of partial shading the resulting development of "hot spots" may thermally destroy modules.[9] Therefore, detecting these shunts is important for qualifying solar cells for their use in solar modules. Very often but not always (see below), non-linear shunts are also pre-breakdown sites.

An established technique to detect and to quantify all kinds of shunts is lock-in thermography (LIT).[7,8,10] In the basic version of this technique, a pulsed bias is applied to the solar cell in the dark ("dark lock-in thermography;" DLIT), and the local temperature modulation caused by the shunt current is used to image the shunts. By variation of the bias applied

* Correspondence to: Otwin Breitenstein, Max-Planck-Institut für Mikrostrukturphysik, Weinberg 2, D-06120 Halle, Germany.
†E-mail: breiten@mpi-halle.mpg.de

Copyright © 2007 John Wiley & Sons, Ltd.

during several DLIT measurements, different types of shunts can be distinguished from each other. For example, linear shunts are characterized by almost identical thermal signals for the same small bias applied in forward or reverse direction, respectively. If LIT is performed by pulsed light irradiation under open circuit conditions (''illuminated lock-in thermography under open circuit,'' V_{OC}-ILIT[11]), the resulting image reveals both inhomogeneities of the local lifetime and local shunts. The detection limit of DLIT for shunts is extremely low. Local shunts with a current of less than 100 μA can easily be detected under forward bias.[10] Because DLIT can be performed at sufficiently small forward bias local variations in the lifetime do not contribute to the measured signal and as a result only the shunts are measured. If samples are imaged without black IR-emitting foil, the infrared emissivity is dominated by the screen-printed Al back contact, which shows a sufficiently high and homogeneous emissivity of about 0·5. Only if shunts below grid lines shall be investigated, special measures to homogenize the emissivity are necessary.

In this work, differently shunted solar cells are imaged by DLIT, V_{OC}-ILIT, PL, and reverse-bias EL in order to investigate the ability of luminescence imaging techniques to localize different shunt types. All LIT images in this work were measured without a black foil at a lock-in frequency between 30 and 40 Hz. The wavelength of the V_{OC}-ILIT excitation was 850 nm, and the illumination intensity was chosen to yield an equivalent short circuit current as measured under 1 sun standard illumination. Hence, the bias for the V_{OC}-ILIT investigation was the open circuit voltage V_{OC}, which is considerably higher than the +0·5 V applied for the DLIT measurement. This was intended, since only V_{OC}-ILIT allows to investigate the cell under high injection conditions without suffering from series resistance problems, whereas DLIT at +0·5 V keeps the cell under low-injection condition and only images linear and non-linear shunts. The PL images in this work were taken with 815 nm illumination and with an illumination intensity equivalent to 0·7 suns. A silicon CCD camera thermoelectrically cooled to −30 degrees Celsius was used for detection of the luminescence signal. For EL measurements two arrays of spring loaded contacting pins were used to contact the busbars homogeneously.

Figure 1 shows the PL, V_{OC}-ILIT, and DLIT images of a standard fully processed, mc silicon solar cell (labeled cell no. 1), which contains weak shunts. This cell was broken (bottom right corner), which however did not prevent its investigation. There is a striking similarity between the PL image (a) and the V_{OC}-ILIT image (b): bright regions in (b) correspond to dark regions in (a) and *vice versa*, with the exception of a shunt (bright spot) in the upper left corner of (b), which is not visible in (a). The forward and reverse bias DLIT images of this cell measured at ±0·5 V are shown in Figures 1c,d, respectively. The quantitative correlation between these two DLIT images allows most of the shunts observed in cell no. 1 to be identified as linear shunts. A few shunts, however, appear only under forward bias, which is a fingerprint of a non-linear shunt. An example is seen at the upper left corner and is marked in Figure 1c by an arrow. This shunt is most probably caused by a recombination-active defect crossing the pn-junction. The linear shunts appear in a region parallel to the left and to the upper edge of the cell, which suggests that this wafer was cut from an ingot located near the outer edges of the casting block. The PL image shows areas of reduced PL intensity (i.e., of reduced minority carrier lifetime) near the top right corner, in the large broken piece at the lower right of the cell, and close to the left, upper, and right edges. The PL image does not clearly show the shunts seen in DLIT, hence the dark areas in PL are low lifetime regions. Some shunts visible in Figures 1c,d are showing up as dark features in the PL image, but an unambiguous distinction of these shunts from, e.g., recombination-active grain boundaries is not possible based on a single PL image.[3] By applying +0·5 V to the cell, the total current through the whole cell is 193 mA. Under reverse bias at −0·5 V the total current is 115 mA. By using quantitative measurements of shunt currents (for details see Reference [8]), the current across all the shunts under forward bias was estimated to be 90 mA, which is close to the 115 mA reverse current. Since the number of these shunts is exceeding 75, the average current across each shunt is in the order of 1·2 mA.

The PL and DLIT images of another mc silicon solar cell (labeled cell no. 2), shown in Figure 2, show a group of strong linear shunts on the left side and two point-like linear shunts in the upper middle part of the cell (marked by white rectangles). We will use the images taken on this cell to determine a rough estimate of the limiting value for point like shunts that can be identified in single PL images.

The DLIT image at −0·5 V reverse bias of cell no. 2 is not shown here, because it shows the same signals as the DLIT image at +0·5 V forward bias. The forward current of that cell under +0·5 V was 285 mA and at −0·5 V reverse bias the current was 245 mA. A quantitative evaluation of the DLIT results[8] shows that

Copyright © 2007 John Wiley & Sons, Ltd.

DOI: 10.1002/pip

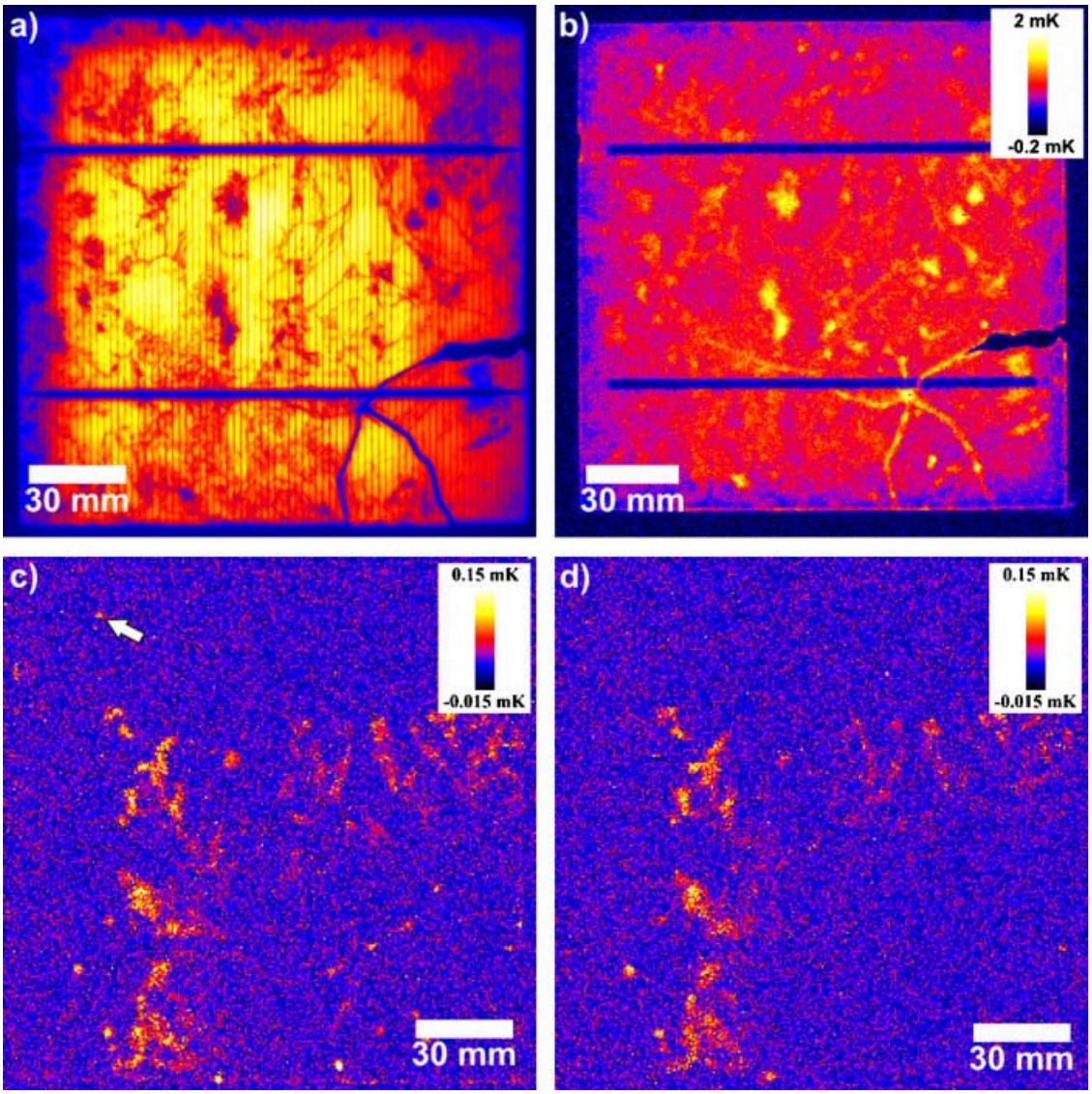

Figure 1. PL image (a), V_{OC}-ILIT image at 1 sun (b), forward DLIT image at $U = +0{\cdot}5$ V (c), and reverse DLIT image at $U = -0{\cdot}5$ V (d) of the cell no. 1, which shows weak shunts. The cell area is $156 \times 156\,mm^2$. The arrow in (c) marks a non-linear shunt.

the current across the dominant group of shunts and the two point-like shunts is 150 mA. Since there are 10 shunts in the whole cell, the average current across each of these shunts was about 15 mA. Of course, not all shunts have exactly the same shunt resistance. According to the DLIT signal height, the single shunt currents vary by a factor of 3–4. One aim of this paper is to determine the order of magnitude of the detection limit of PL imaging for shunt analysis. An exact value of this detection limit cannot be given, since it depends not only on the parameters of the PL measurement but also on the presence of other defects in the cell and on the exact cell properties. For example, for monocrystalline cells, which do not contain any grain boundaries, PL may detect weaker shunts than for mc cells.[5] It is also important to note that the visibility of shunts in luminescence images is a lateral series resistance effect caused by lateral current flow into the shunt. The shunt detection limit thus critically depends on the resistivity along the lateral current path, which is determined by the emitter conductivity and by the layout and conductivity of the metal contacts.

In the absence of shunts, the PL image of mc cells is dominated by the recombination activity of the grain

Copyright © 2007 John Wiley & Sons, Ltd.

DOI: 10.1002/pip

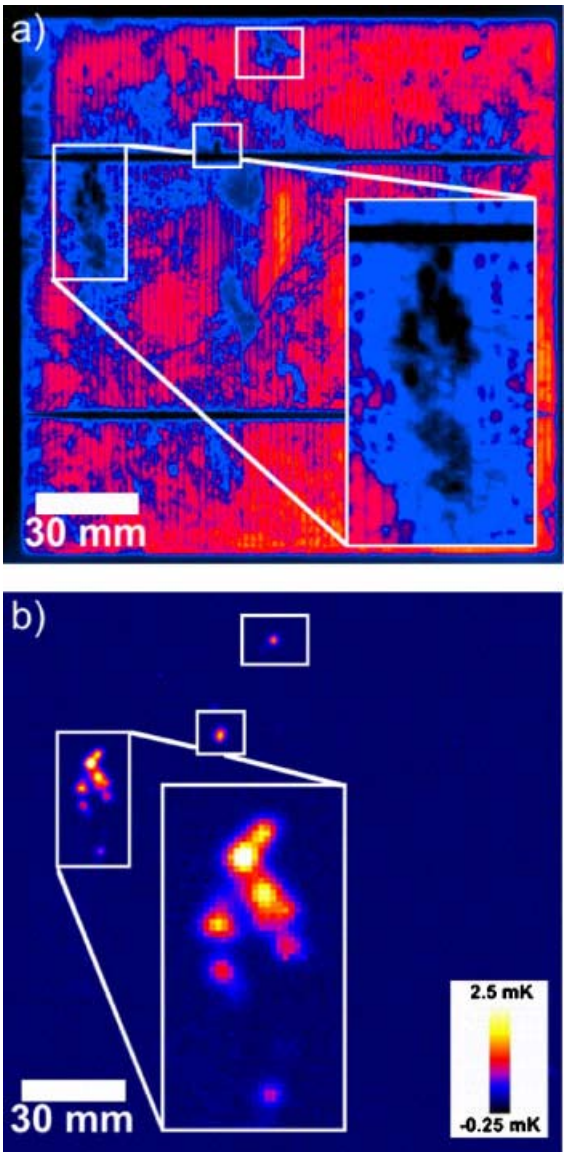

Figure 2. PL image (a), and forward bias DLIT image at $U = +0{\cdot}5$ V (b) of cell no. 2, which contains stronger shunts. The shunts are visible in the PL image and are marked by white rectangles. The cell area is $156 \times 156\,\mathrm{mm}^2$.

boundaries.[2,3,4] In the PL image in Figure 2a very dark areas appear at the positions of the shunts. A close-up of the dominating group of shunts is shown in the inset of Figure 2a. In comparison to other areas of reduced intensity the PL signals from the shunted regions are particularly low, they have a circular or elliptic shape, and are blurry at their edges. This blurring effect has been reported previously[3,4] and is a result of the lateral current flow: under illumination, non-shunted regions are biased to the open circuit voltage V_{OC}. Shunted regions are connected to the non-shunted regions in parallel, causing lateral current flow into the shunt under illumination. The voltage losses associated with these lateral currents result in reduced voltages and thus reduced luminescence intensity in the vicinity of the shunt. The spatial extension of the dark areas around the shunts is governed by the lateral sheet resistance in the emitter and the metal fingers, the strength of the shunt, and the light intensity. A full quantitative theoretical analysis of these effects is beyond the scope of this paper.[12] By comparing the PL image with the DLIT image in Figure 2, one generally observes good agreement of the shunt positions, i.e., very dark blurred spots in PL correspond to bright spots in DLIT. However, this agreement is not complete. For example, in the lower part of the left highlighted region there are two dark spots in the PL image, but only the lower (and darker) of them is a shunt. Hence strong linear shunts are reliably detectable in single PL images. However, in a certain range of the shunt currents and without the DLIT images for comparison it can be difficult to distinguish between dark areas in the PL image that are caused by shunts and dark areas, which have another origin. The average shunt current of about 15 mA at $\pm 0{\cdot}5$ V for the point-like shunts estimated here just marks the order of magnitude of a limit, above which single shunts are clearly detectable in single PL images. As mentioned before, in monocrystalline silicon solar cells with more homogeneous material quality, weaker shunts will be identifiable reliably.[5]

An example of so-called pre-breakdown sites can be seen in another mc solar cell (labeled cell no. 3) shown in Figure 3. In this cell only a small group of shunts is visible at the right edge under forward bias of $+0{\cdot}5$ V, see Figure 3a. These shunts are not visible under small reverse bias direction at $-0{\cdot}5$ V as shown in Figure 3b, hence these are typical non-linear shunts. However, if one applies a reverse voltage of -6 V to the cell, strong DLIT signals appear at the position of these shunts and also in other positions of the cell, as shown in Figure 3c. In Figure 3c the 0°- (in-phase-) image of the DLIT measurement is shown, because in this image the shunts are visible with a higher spatial resolution than by the DLIT amplitude image.[10] These shunts are typical pre-breakdown sites. The total current at -6 V reverse bias was $2{\cdot}85$ A, at slightly higher reverse bias it exceeds 5 A. Hence these shunts, while not affecting the cell efficiency under 1 sun, are potential sources of hot spots under reverse bias and thus dangerous for a module.

Since PL does not allow an investigation under reverse bias, EL under reverse bias was used to detect the

Copyright © 2007 John Wiley & Sons, Ltd.

DOI: 10.1002/pip

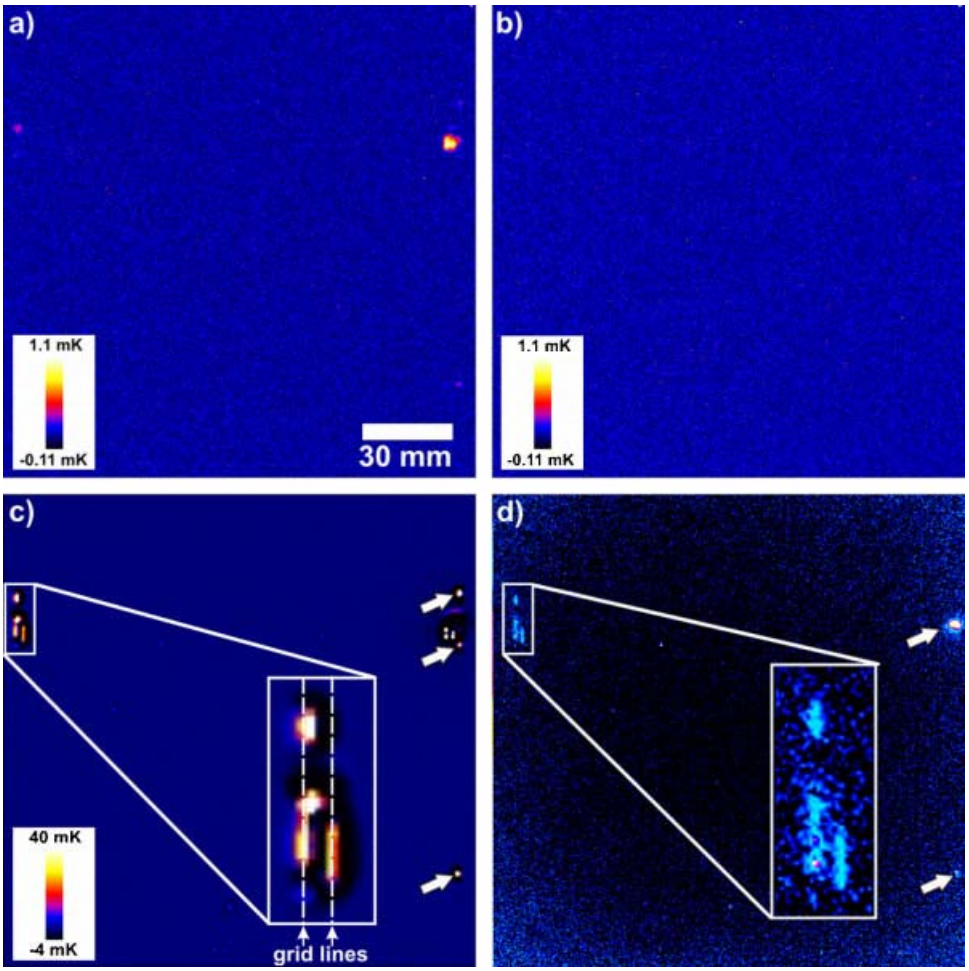

Figure 3. Pre-breakdown sites in a $156 \times 156\,mm^2$ solar cell (cell no. 3). Forward bias DLIT image at $+0{\cdot}5$ V (a), reverse bias DLIT image at $-0{\cdot}5$ V (b), reverse bias DLIT image at -6 V (c), and EL image at -2 A reverse current (d). The scale bar in (a) holds for all images of this figure.

pre-breakdown sites by luminescence. An EL image of the cell no. 3 was taken in the dark with -2 A reverse current (at ≈ -5 V). This image is shown in Figure 3d. We observe a good correlation between the pre-breakdown signals of the DLIT measurement (Figure 3c) and the EL image. On the left edge of the cell three extended pre-breakdown sites appear. These line-shaped sites are possibly caused by an extremely thin emitter in that area, causing the silver grid to be in contact with the p-type substrate of the cell. Here the silver grid would make a Schottky-contact to the base, which breaks down under reverse bias. This hypothesis corresponds to the observation that the pre-breakdown sites appear exactly along the metal grid fingers, as shown in the inset of Figure 3c. Further line-shaped pre-breakdown sites at grid lines appear at the right edge of this cell, as shown in the DLIT image 3c. However, these shunts do not appear in the reverse bias EL image Figure 3d. In addition, the DLIT image shows three point-like pre-breakdown sites, which are marked by arrows in Figure 3c. Only the lowest one is also visible in the reverse bias EL image. The upper right EL spot in Figure 3d is lying in between the pre-breakdown sites in this region. The breakdown mechanism of the point-like sites, which are marked by arrows in Figures 3c,d, is not clarified yet. Photon emission from reverse-biased silicon pn-junctions,[13] or from avalanche breakdowns[14] are possible explanations.

Not all of the pre-breakdown sites are thus visible in reverse bias EL, which indicates that there are different types of pre-breakdown sites in silicon solar cells. However, at least some pre-breakdown sites are well detectable by EL, and the measurements show a good correlation with DLIT investigations.

Copyright © 2007 John Wiley & Sons, Ltd.

DOI: 10.1002/pip

LIT images of mc silicon solar cells were compared with luminescence images of the same cells to test the ability of PL and reverse-bias EL measurements for detecting shunts. By comparing DLIT images of silicon solar cells containing weak, moderate, and strong linear and non-linear shunts with PL images of the same cells, we find that weak shunts cannot unambiguously be localized in single PL images. However, stronger linear shunts are visible in PL images. As a criteria describing the strength of a shunt we choose the current per shunt measured at +0·5 V forward bias, which is close to the operating point of the cell. By quantitatively evaluating the DLIT images of the cells, we can calculate an approximate value for the average current per shunt for different solar cells. The current limit for detecting point like shunts with the PL method was determined to be in the order of 15 mA per shunt in mc-Si solar cells. This means that PL signals that are caused by shunts with considerably less than 15 mA/shunt are difficult to distinguish in mc-Si solar cells from other defects or are not detectable at all. Linear shunts, which are considerably stronger than 15 mA/shunt are clearly detectable by PL. Pre-breakdown sites were detectable with EL if performed under reverse bias, and we obtained a good correlation between DLIT and EL images, respectively. However, not all pre-breakdown sites were visible in reverse-bias EL.

Acknowledgements

The authors thank Deutsche Cell GmbH in Freiberg, Germany, and Q-Cells AG in Thalheim, Germany, for providing the solar cells investigated in this study. This work was supported by the German Ministry for Environment (BMU) under contract no. 0327650D (SolarFocus). The Centre of Excellence for Advanced Silicon Photovoltaics and Photonics is funded under the Australian research Council's Centres of Excellence Scheme.

REFERENCES

1. Fuyuki T, Kondo H, Yamazaki T, Takahashi Y, Uraoka Y. Photographic surveying of minority carrier diffusion length in polycrystalline silicon solar cells by electroluminescence. *Applied Physics Letters* 2005; **86**: 262108. DOI: 10.1063/1.1978979.
2. Trupke T, Bardos RA, Schubert MC, Warta W. Photoluminescence imaging of silicon wafers. *Applied Physics Letters* 2006; **89**: 044107. DOI: 10.1063/1.2234747.
3. Kasemann M, Schubert MC, The M, Köber M, Hermle M, Warta W. Comparison of luminescence imaging and illuminated lock-in thermography on silicon solar cells. *Applied Physics Letters* 2006; **89**: 224102. DOI: 10.1063/1.2399346.
4. Trupke T, Bardos RA, Abbott MD, Fisher K, Bauer J, Breitenstein O. Luminescence imaging for fast shunt localization in silicon solar cells and silicon wafers. *International Workshop on Science and Technology of Crystalline Silicon Solar Cells*, Sendai, Japan, October, 2006 (proceedings in print).
5. Bothe K, Pohl P, Schmidt J, Weber T, Altermatt PP, Fischer B, Brendel R. Electroluminescence imaging as an in-line characterization tool for solar cell production. In *Proceeding of the 21st European Photovoltaic Solar Energy Conference*, Dresden, Germany, 2006; 597–600.
6. Abbott MD, Trupke T, Hartmann HP, Gupta R, Breitenstein O. Laser isolation of shunted regions in industrial solar cells. *Progress in Photovoltaics: Research and Applications* 2007; **15**: 613–620. DOI: 10.1002/pip.766.
7. Breitenstein O, Langenkamp M, Rakotoniaina JP, Zettner J. The imaging of shunts in solar cells by infrared lock-in thermography. In *Proceedings of the 17th European Photovoltaic Solar Energy Conference*, Munich, Germany, 2001; 1499–1502.
8. Breitenstein O, Rakotoniaina JP, Al Rifai MH. Quantitative evaluation of shunts in solar cells by lock-in thermography. *Progress in Photovoltaics: Research and Applications* 2003; **11**: 515–526. DOI: 10.1002/pip.520.
9. Herrmann W, Alonso MC, Boehmer W, Wambach K. Effective hot-spot protection on PV modules—characteristics of crystalline silicon cells and consequences for cell production. In *Proceedings of the 17th European Photovoltaic Solar Energy Conference*, Munich, Germany, 2001; 1646–1649.
10. Breitenstein O, Langenkamp M. *Lock-in Thermography—Basics and Use for Functional Diagnostics of Electronic Components*. Springer: Berlin, Heidelberg, 2003.
11. Isenberg J, Warta W. Realistic evaluation of power losses in solar cells by using thermographic methods. *Journal of Applied Physics* 2004; **95**: 5200–5209. DOI: 10.1063/1.1690103.
12. Kasemann M, Augarten Y, Trupke T, Bardos R, Warta W. Shunt detection capabilities of luminescence imaging on silicon solar cells. *To be Presented at 22nd European Photovoltaics Solar Energy Conference*, Milan, Italy, September 2007.
13. Obeidat AT, Kalaylian Z, Andreou AG, Khurgin JB. A model for visible photon emission from reverse-biased silicon p-n junctions. *Applied Physics Letters* 1997; **70**: 470–471.
14. Chynoweth AG, McKay KG. Photon emission from avalanche breakdown in silicon. *Physical Review* 1956; **102**: 369–376.

Copyright © 2007 John Wiley & Sons, Ltd.